

**Local quantum criticality of a one-dimensional Kondo insulator model**W. Zhu<sup>1</sup> and Jian-Xin Zhu<sup>1,2</sup><sup>1</sup>*Theoretical Division, T-4 and CNLS, Los Alamos National Laboratory, Los Alamos, New Mexico 87545, USA*<sup>2</sup>*Center for Integrated Nanotechnologies, Los Alamos National Laboratory, Los Alamos, New Mexico 87545, USA*

(Received 29 January 2018; revised manuscript received 15 May 2018; published 13 June 2018)

The continuous quantum phase transition and the nature of the quantum critical point (QCP) in a modified Kondo lattice model with Ising anisotropic exchange interactions are studied within the density-matrix renormalization group algorithm. We investigate the effect of quantum fluctuations on critical Kondo destruction QCP by probing static and dynamic properties of the magnetic order and the Kondo effect. In particular, we identify that local Kondo physics itself becomes critical at the magnetic phase transition point, providing unbiased evidences for local quantum criticality between two insulators without involving the Fermi surface.

DOI: [10.1103/PhysRevB.97.245119](https://doi.org/10.1103/PhysRevB.97.245119)**I. INTRODUCTION**

Quantum criticality describes the collective fluctuations of matter undergoing a continuous phase transition at zero temperature [1]. As quantum criticality is central to a broad understanding of strongly correlated quantum matter, how to properly describe the physics around quantum critical points (QCPs) is a subject of intensive research [2]. Experimentally, the intermetallic heavy-fermion compounds [3–5] serve as ideal candidates for the study of quantum phase transitions and criticalities by exhibiting unusual properties, such as heavy Fermi liquid, magnetic ordering, as well as unconventional superconductivity [6]. In addition, a continuous suppression of antiferromagnetic transition temperature has been discovered in a sizable number of (nearly) stoichiometric heavy-fermion systems [2].

For QCPs relevant to the heavy-fermion systems, two major theoretical scenarios have been proposed: One is the spin-density-wave QCP [7,8] and the other one is critical Kondo destruction QCP [9–11]. For spin-density-wave QCP, conduction electrons acquire peculiar dynamics through an essentially perturbative coupling to the slow critical modes of magnetic background. While in the latter case the local Kondo physics itself becomes critical at the magnetic ordering transition, thus a local QCP is driven by the competition between local dynamics and long-ranged magnetic fluctuations. So far, despite considerable efforts, debate continues on the nature of QCP, and several issues remain elusive in the heavy-fermion systems. First, it is generally believed that the spin fluctuations in three dimension leads to a Doniach's QCP [12,13] with dynamical spin susceptibility satisfying usual Fermi-liquid form, while two-dimensional spin fluctuations tend to favor local QCP with spatially extended critical degrees of freedom coexisting at the critical point [9]. Much less is known about what kind of QCP in a one-dimensional heavy-fermion system could follow. Second, a key assumption to distinguish different scenarios usually resorts to the abrupt shrink of the Fermi surface when across a local QCP [6]. Although the argument of the Fermi surface in a metallic phase is natural [14–18], the QCP connecting two insulators without a Fermi surface has been hardly explored before, raising the

question of whether or not the change of Fermi surface is associated with the local QCP. Third, all of the previous characterizations of local QCP in heavy-Fermi metals are based on the extended dynamical mean-field theory (EDMFT) [9,19–24] or large- $N$  [25,26] approaches. In these approaches, the spatial and temporal quantum fluctuations are either partially or completely neglected, which is valid in high dimension. Therefore, an unbiased and controlled numerical method to capture the full quantum fluctuations of local moments and itinerant electrons, which become particularly important in low-dimensional systems, is highly desired to clarify the nature of QCP.

The aim of this paper is to address the aforementioned problems and provide compelling numerical evidences for locally critical phase transitions in a microscopic one-dimensional Kondo lattice model (KLM). Based on the density-matrix renormalization group (DMRG) calculations, we are able to access the low-lying energy excitations, static and dynamical correlations of local moments, as well as the charge degree of freedom. We first identify a continuous phase transition between Kondo insulator and antiferromagnetic (AFM) phases, signaled by the closing neutral gap and various magnetic order parameters such as magnetization. We then demonstrate the evolution of local susceptibility across the magnetic phase transition. The singular behavior indicates the Kondo screening being critical at the transition point, serving as the hallmark of local quantum criticality. These results provide compelling evidence of local QCP between two insulators without involving the Fermi surface, which indicates that the notion of local QCP as a general paradigm for novel phase transitions, is not limited to heavy-fermion metals [6,9]. We hope this work could stimulate the study of heavy-fermion quantum criticality in one dimension. The experimental realization of one-dimensional heavy-Fermi-system  $\text{CeCo}_2\text{Ga}_8$  compounds [27] could provide a platform to test our proposal.

**II. MODEL AND METHOD**

We consider a modified Kondo lattice model in one dimension with an additional Ising-type interaction between the local spins (Fig. 1), where each unit cell contains a localized spin

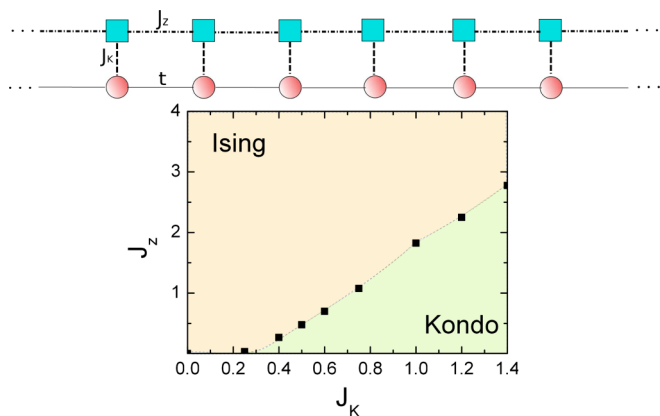


FIG. 1. (Top) One-dimensional Kondo lattice model with an Ising-type interaction between nearest-neighbor localized spins. Red dots and blue squares represent the conduction electrons and localized spins, respectively. (Bottom) The global phase diagram as a function of  $J_z$  and  $J_K$  by setting  $t = 0.25$  (bandwidth of conduction electron is  $4t = 1$ ). The phase transition is determined to be continuous (see main text).

and an extended conduction-band electron state:

$$H = t \sum_{(ij),\sigma} c_{i\sigma}^\dagger c_{j\sigma} + J_K \sum_i \mathbf{S}_i \cdot \mathbf{s}_i + J_z \sum_{(ij)} S_i^z S_j^z. \quad (1)$$

Here  $c_{i\sigma}^\dagger$  ( $c_{i\sigma}$ ) denotes the creation operator of a conduction electron with spin  $\sigma = \uparrow, \downarrow$  at site  $i$ . The  $\mathbf{S}_i$  is a localized moment with  $S = \frac{1}{2}$ . Each localized moment interacts via an exchange coupling  $J_K$  with the conduction electron, where the conduction electron density is defined as  $\mathbf{s}_i = \frac{1}{2} \sum_{\sigma,\sigma'} c_{i\sigma}^\dagger \vec{\sigma}_{\alpha\beta} c_{i\sigma}$ . The quantity  $J_z$  describes the Ising-type magnetic exchange interaction between the low moments [28]. We note that the magnetic exchange interaction is usually generated by the Kondo interaction via the Ruderman-Kittel-Kasuya-Yosida (RKKY) effect. Here we have treated it as an independent parameter for two reasons. First, it helps the purpose of specifying the global phase diagram. Second, in one dimension, the Heisenberg-type RKKY interaction always preserves the spin-rotational invariance while the Ising interaction could stabilize AFM order [29]. Therefore, the KLM with Ising-type exchange interaction has the advantage of ameliorating the double-counting issue arising from an explicit inclusion of the intrinsic RKKY-based exchange interaction, the latter requiring a treatment of conduction electrons with care [30]. Experimentally, the easy-axis anisotropy widely exists in a number of heavy-fermion systems [31]. Physically, two important mechanisms compete with each other [12,13]: An isolated local moment would be screened by the spins of conduction electrons through the Kondo screening, while the magnetic exchange interaction tends to induce a long-ranged magnetic ordering. In the absence of Ising-type interaction, the ground state of KLM (at half filling) is spin singlet and the spin gap always exists for any finite exchange  $J_K$ , supported by both semiclassical analysis [32] and finite-size numerical calculations [33–36]. In the regime where Ising-type exchange interaction dominates, the AFM phase is expected. Therefore, we expect a magnetic phase transition from the

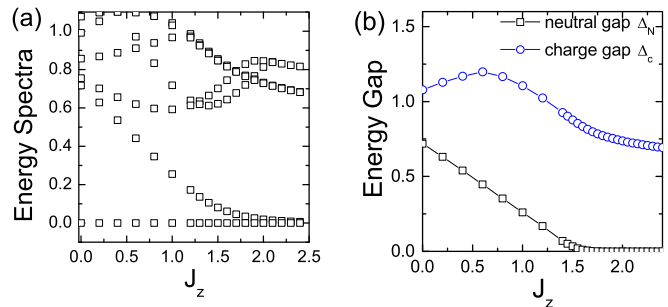


FIG. 2. (a) Energy spectrum evolution as a function of  $J_z$ , obtained on an  $L = 8$  periodic chain by ED calculations. (b) Energy gaps ( $\Delta_S$ ,  $\Delta_N$ ,  $\Delta_C$  defined in main text) as a function of  $J_z$ , obtained on  $L = 36$  open chain by DMRG calculations. Here we set  $J_K = 1.0$ .

nonmagnetic phase to the AFM phase driven by the Ising exchange interaction.

In this work, we study the KLM as described by Eq. (1) using the exact diagonalization (ED) and density-matrix renormalization group (DMRG) method [37]. In DMRG calculations, we use the finite system algorithm with open boundary conditions for system size up to  $L = 72$ . We use two different  $U(1)$  quantum numbers in the DMRG setup. One is the total electron numbers  $N^e = n_\uparrow + n_\downarrow$ , including number of spin- $\uparrow$   $n_\uparrow$  and spin- $\downarrow$   $n_\downarrow$  electrons, and the other one is the  $z$  component of total spin  $I^z = (n_\uparrow - n_\downarrow)/2 + S^z$ , where  $S^z$  is the  $z$  component of the total local moments. To study the Kondo insulator we restrict ourselves to half-filling where the total number of conduction electrons  $N^e$  equals number of sites  $L$ , or the average occupancy is 1 (half filling). The dynamical response functions are computed within the scheme of dynamical DMRG [38,39]. By keeping up to 640 states, the truncation error is controlled below  $<10^{-9}$  for static properties and  $<10^{-6}$  for dynamical susceptibility calculations, respectively.

### III. NUMERICAL RESULTS

We first present numerical evidences of Ising-anisotropy-driven phase transition, based on the low-lying energy spectrum from ED calculation. As shown in Fig. 2(a), there exists a doublet ground-state manifold in the large- $J_z$  regime related to the AFM ground states in the Ising limit, while the single ground state in the small- $J_z$  regime corresponds to the ground-state-enclosing spin singlet between a localized spin and one conduction electron state on each lattice site. In particular, upon decreasing  $J_z$ , one energy level is continuously gapped out from the ground-state manifold, signaling a second-order-type phase transition. Here, the ED energy spectrum presents the unambiguous evidence of a continuous phase transition from an AFM ordered phase to a nonmagnetic Kondo insulator phase by tuning down the Ising exchange interaction  $J_z$ , whose nature will be addressed by DMRG calculations on the system of large sizes as below.

Further evidences of a continuous phase transition can be obtained by DMRG calculations for larger system sizes. Here we define two different energy gaps. First, the energy difference between the ground state and lowest excited state with the same quantum numbers  $N^e, I^z$ :  $\Delta_N = E_1(N^e = L, I^z = 0) - E_0(N^e = L, I^z = 0)$ , is defined as the neutral gap. Second,

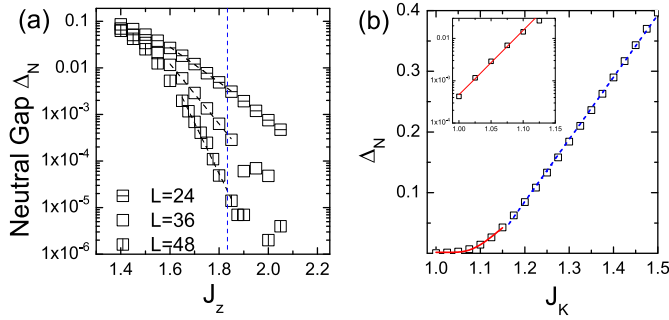


FIG. 3. (a) Log-linear plot of neutral gap  $\Delta_N$  near the critical point  $J_z^c \approx 1.825$  by setting  $J_K = 1.0$ . Various system sizes are labeled by different symbols. (b) Neutral gap  $\Delta_N$  as a function of  $J_K$  by setting  $J_z = J_z^c = 1.825$ . Inset: Log-linear plot of  $\Delta_N$  and exponential fitting.

the charge gap is obtained by the energy difference between the ground state and lowest excited state with different electron number  $\Delta_C = E_0(N^e = L + 2, I^z = 0) - E_0(N^e = L, I^z = 0)$ . The evolution of energy gaps as a function of  $J_z$  is shown in Fig. 2(b). By tuning up  $J_z$ , the neutral gap starts to monotonically decreases to zero. In the whole process, the charge gap is always open. The neutral gap continuously goes to zero, supporting a second-order phase transition driven by the Ising anisotropy from the Kondo insulator to an Ising AFM insulating phase.

It is worth mentioning that the neutral gap shows exponential behavior by approaching the critical point, while away from the critical point the neutral gap is linearly dependent on  $J_z$ . As shown in Fig. 3(a), when  $J_z$  approaches the critical point, the neutral gap is found to behave as exponentially decayed, for all system sizes. Similarly, by tuning  $J_K$ , the neutral gap respectively shows exponential dependence and linear dependence near the critical point and away from the critical point. The exponential dependence of the energy scale near the critical point is a signature of the Kondo physics becoming critical.

The phase transition can be described by several local order parameters, as shown in Fig. 4. First, the magnetic order parameter  $m_{AF} = \frac{1}{L} \sum_i |\langle S_i^z \rangle|$  develops continuously as  $J_z$  exceeds the critical point  $J_z^c$ . Importantly, we observe that the charge degree of freedom shows very similar behavior

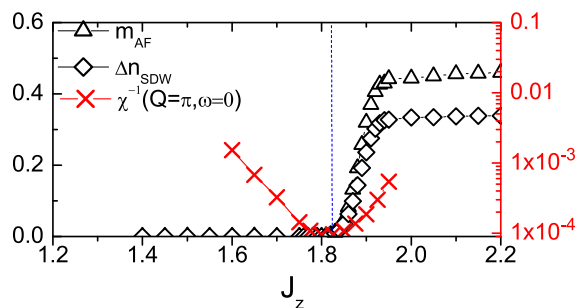


FIG. 4. Antiferromagnetic order parameter  $m_{AF} = \frac{1}{L} \sum_i |\langle S_i^z \rangle|$  (black triangular) and spin-density-wave order parameter  $\Delta n_{SDW} = \frac{1}{L} \sum_i |\langle s_i^z \rangle|$  (black diamond), and inverse static spin susceptibility  $1/\chi(Q = \pi, \omega = 0)$  (red cross) as a function of  $J_z$ . Blue dashed line marks the transition point  $J_z^c \approx 1.825$ .

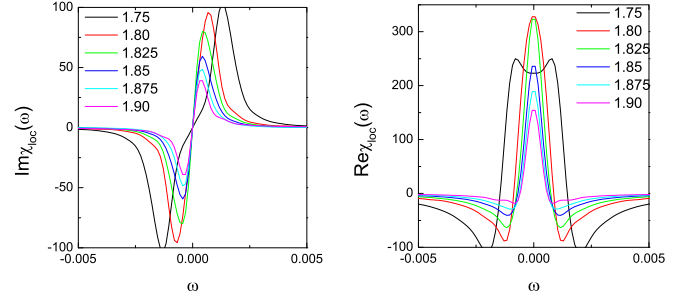


FIG. 5. Frequency dependence of the local spin susceptibility at various values of  $J_z$  around the magnetic transition: (left panel) imaginary part and (right panel) real part. Here we choose  $J_K = 1.0$ .

with local moments. Within the numerical uncertainty, the spin-density wave pattern ( $\Delta n_{SDW} = \frac{1}{L} \sum_i |\langle s_i^z \rangle|$ ) always occurs simultaneously with nonzero magnetization  $m_{AF}$ . This excludes the possibility of a spin-density-wave-driven phase transition. In addition, a magnetic phase transition can also be probed by lattice static susceptibility at a magnetic wave vector. The lattice static susceptibility is defined as  $\chi(Q, \omega) = -i \int dt e^{i\omega t} \langle [S_Q^z(t), S_Q^z(0)] \rangle$ , where  $S_Q^z = \frac{1}{L} \sum_n \sin(\frac{\pi n}{L+1}) S_n^z$  with  $n$  being the site index. As shown in Fig. 4, the inverse lattice static susceptibility at the magnetic wave vector  $\chi^{-1}(Q = \pi, \omega = 0)$  reaches a minimum at the transition point determined by  $m_{AF}$  and  $\Delta n_{SDW}$ . The order parameters, including lattice static susceptibility, magnetization, and charge density imbalance, point to a continuous phase transition between the Kondo insulator and the AFM insulator, and determine the magnetic critical point unambiguously.

To uncover the nature of this phase transition, we further investigate the local dynamical response function. For this purpose, we introduce the local spin susceptibility, which is defined as

$$\chi_{loc}(\omega) = \langle 0 | \Delta S_j^z \frac{1}{\omega - (E_0 - H) + i\eta} \Delta S_j^z | 0 \rangle \quad (2)$$

and  $\Delta S_j^z = S_j^z - \langle S_j^z \rangle$ . (We choose site  $j$  in the center of the chain.) Figure 5 shows the local spin susceptibility around the quantum critical point. In the Kondo singlet phase  $J_z < J_z^c$ , the peak of  $\Im \chi_{loc}(\omega)$  stands away from the zero frequency, consistent with the gapped spin excitations. As  $J_z$  increases, the dominant peak moves towards the low frequency and reaches zero frequency around  $J_z \approx J_z^c$ . Near the critical point

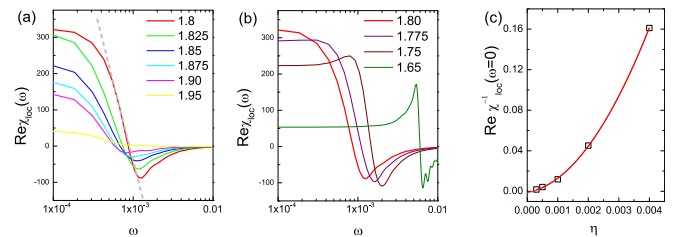


FIG. 6. Semilog plot of the real part of the local spin susceptibility around the magnetic transition: (a)  $J_z > J_z^c$  and (b)  $J_z < J_z^c$ . (c) Inverse of the real part of the local spin susceptibility  $\Re \chi^{-1}(\omega = 0)$  versus  $\eta$ . Red line shows the polynomial function fitting:  $\Re \chi^{-1}(\omega = 0) = A\eta^2 + B\eta + C$ , with nonzero  $A$ ,  $B$ , and  $C = -0.0013 \pm 0.002$ .

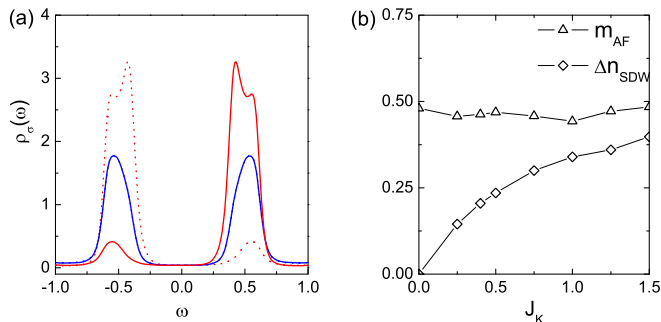


FIG. 7. (a) Local electron spectrum density as a function of  $\omega$  for  $J_z = 1.65$  (blue) and  $J_z = 1.95$  (red). Solid and dotted line represents spin-down and spin-up component, respectively. (b) In the Ising AFM phase, the  $J_K$  dependence of magnetization  $m_{AF}$  and charge polarization  $\Delta n_{SDW}$ . The parameter  $J_z$  is set to be  $J_z = J_K + 1$ .

$J_z^c$ ,  $\Re\chi_{loc}(\omega = 0)$  becomes steeper, which leads to a peak structure developing at  $\Re\chi_{loc}(\omega = 0)$ . The maximal value of  $\Re\chi_{loc}(\omega = 0)$  defines the critical point  $J_z^c$ . Since the singular behavior  $\Re\chi_{loc}(\omega)$  at around zero frequency is key to the nature of QCP, we inspect the  $\Re\chi(\omega)$  in detail in Fig. 6. We show the semilogarithmic plot of  $\Re\chi_{loc}(\omega)$  with a focus on the low-frequency regime. It is found that, for the Kondo insulator phase  $J_z < J_z^c$ ,  $\Re\chi_{loc}(\omega \rightarrow 0)$  saturates to a finite value in the low-frequency limit [Fig. 6(b)]; however, around the critical point  $J_z \approx J_z^c$ ,  $\Re\chi_{loc}(\omega \rightarrow 0)$  shows distinct behavior. To demonstrate the singular behavior of  $\Re\chi_{loc}(\omega = 0)$ , we investigate the  $\Re\chi_{loc}(\omega = 0)$  dependence on  $\eta$ , which is the imaginary part in the dynamical response function Eq. (2). To the best fit, we determine that the inverse of  $\Re\chi_{loc}(\omega = 0)$  has a polynomial dependence on  $\eta$  [Fig. 6(c)]. In the intrinsic limit ( $\eta \rightarrow 0$ ), we determine that  $\Re\chi_{loc}^{-1}(\omega = 0)$  is scaled to zero within the fitting accuracy, and thus  $\Re\chi_{loc}(\omega = 0)$  becomes singular. Physically, the divergence of local susceptibility signals the Kondo screening being critical, which is the hallmark of local quantum criticality [6,9]. Here we emphasize that, compared with previous studies [22–24], the advantage of the current scheme is that we can target the behavior at zero frequency  $\Re\chi_{loc}(\omega = 0)$  directly, instead of relying on extracting the scaling behavior first in the low frequency. An additional support for critical local physics is provided by a logarithmically scaling form [9]:  $\Re\chi_{loc}(\omega) \approx \alpha \ln|\omega|^{-1}$  within the energy window  $T_K^* < \omega < T_K^0$ , where the effective Kondo scale  $T_K^*$  vanishes logarithmically slowly as approaching the critical point  $J_z \rightarrow J_z^c$ . In Fig. 6(a), we show such scaling behavior indeed emerges in the vicinity of zero frequency (gray dashed line).

One more advantage of our method is to treat the spin and charge degrees of freedom on an equal footing. Here we show the electron spectrum density  $\rho_\sigma(\omega) = \frac{1}{L} \sum_i \rho_{i\sigma}(\omega)$  around the phase transition in Fig. 7(a), where  $\rho_{i\sigma}(\omega) = -\frac{1}{\pi} \Im \langle 0 | c_{i\sigma} \frac{1}{\omega - (E_0 - \hat{H}) + i\eta} c_{i\sigma}^\dagger | 0 \rangle$ . In the Kondo insulator phase ( $J_z = 1.65 < J_z^c$ ), the electron density is uniformly distributed

in real space and the spectrum density is gapped with equal weight below and above the Fermi energy. In the AFM phase ( $J_z = 1.95 > J_z^c$ ), the spin-density wave pattern is formed in real space, which results in an imbalance of the spectral weight of the spin-resolved spectral density in the lower and upper gap edges. In particular, the gap around the Fermi energy in the spectrum density remains open as  $J_z$  crosses the critical point, consistent with the charge gap evolution in Fig. 2(b). This result is in striking contrast to the expectation from the Gutzwiller variational wave function or other auxiliary mean-field methods [40–42], even for the one-dimensional systems where the quasiparticle gap in the conduction electron sector should be closed at the critical point. To further understand this observation we expect that advanced methods could be applied to our model, such as the renormalization group analysis [43]. In addition, we find that in the Ising AFM phase the magnitude of spin polarization  $\Delta n_{SDW}$  strongly depends on  $J_K$ , while the local moment magnetization  $m_{AF}$  is almost unchanged. These facts indicate that the spin-density wave in the conduction electron sector is a “slave” to the local spin AFM order, partially supporting the local critical picture.

#### IV. CONCLUSIONS

We have presented a thorough numerical study of a continuous phase transition between the Kondo insulator and the anti-ferromagnetic phases in a modified Kondo lattice model, which is of great present interest in connection with heavy-fermion quantum criticality. Around the magnetic phase transition point, the magnetic order parameter vanishes continuously and the static susceptibility at the magnetic ordering wave vector diverges. A concomitant divergence of the static local susceptibility signals that the Kondo physics also becomes critical at the quantum critical point. These results provide a “proof-of-the-principle” example that the local quantum criticality [9] can also occur for the transition between two insulating phases, where the Fermi surface becomes irrelevant. This indicates that the local quantum criticality is a general paradigm for novel phase transitions, which is applicable for both heavy-fermion metals [6,9] and heavy-fermion insulators. Moreover, this work not only helps us understand the role of dimensionality in quantum criticality, but also opens a pathway to study novel quantum criticality in one-dimensional heavy-fermion systems. Very soon experimental realization of one-dimensional heavy-Fermi systems [27] could be a test-bed for our proposal.

#### ACKNOWLEDGMENTS

This work was supported by the U.S. DOE at Los Alamos National Laboratory under Contract No. DE-AC52-06NA25396 through the LANL LDRD Program (W.Z.), and the U.S. DOE Office of Basic Energy Sciences (J.-X.Z.). It was supported in part by the Center for Integrated Nanotechnologies, a U.S. DOE Basic Energy Sciences user facility.

[1] S. Sachdev, *Quantum Phase Transitions*, 2nd ed. (Cambridge University Press, Cambridge, UK, 2011).

[2] H. v. Lohneysen, A. Rosch, M. Vojta, and P. Wolfle, *Rev. Mod. Phys.* **79**, 1015 (2007).

- [3] G. R. Stewart, *Rev. Mod. Phys.* **56**, 755 (1984).
- [4] H. Tsunetsugu, M. Sigrist, and K. Ueda, *Rev. Mod. Phys.* **69**, 809 (1997).
- [5] G. R. Stewart, *Rev. Mod. Phys.* **73**, 797 (2001); **78**, 743 (2006).
- [6] P. Genenwart, Q. M. Si, and F. Steglich, *Nat. Phys.* **4**, 186 (2008).
- [7] J. A. Hertz, *Phys. Rev. B* **14**, 1165 (1976).
- [8] A. J. Millis, *Phys. Rev. B* **48**, 7183 (1993).
- [9] Q. Si, S. Rabello, K. Ingersent, and J. L. Smith, *Nature (London)* **413**, 804 (2001).
- [10] T. Senthil, S. Sachdev, and M. Vojta, *Phys. Rev. Lett.* **90**, 216403 (2003).
- [11] P. Coleman and A. H. Nevidomskyy, *J. Low Temp. Phys.* **161**, 182 (2010).
- [12] S. Doniach, *Physica B* **91**, 231 (1977).
- [13] C. M. Varma, *Rev. Mod. Phys.* **48**, 219 (1976).
- [14] J. C. Xavier, E. Novais, and E. Miranda, *Phys. Rev. B* **65**, 214406 (2002).
- [15] S. A. Basylko, P. H. Lundow, and A. Rosengren, *Phys. Rev. B* **77**, 073103 (2008).
- [16] M. Troyer and D. Wurtz, *Phys. Rev. B* **47**, 2886 (1993).
- [17] H. Tsunetsugu, M. Sigrist, and K. Ueda, *Phys. Rev. B* **47**, 8345(R) (1993).
- [18] S. Moukouri and L. G. Caron, *Phys. Rev. B* **54**, 12212 (1996).
- [19] D. R. Grempel and Q. Si, *Phys. Rev. Lett.* **91**, 026401 (2003).
- [20] J.-X. Zhu, D. R. Grempel, and Q. Si, *Phys. Rev. Lett.* **91**, 156404 (2003).
- [21] P. Sun and G. Kotliar, *Phys. Rev. Lett.* **91**, 037209 (2003).
- [22] J.-X. Zhu, S. Kirchner, R. Bulla, and Q. Si, *Phys. Rev. Lett.* **99**, 227204 (2007).
- [23] M. T. Glossop and K. Ingersent, *Phys. Rev. Lett.* **99**, 227203 (2007).
- [24] M. T. Glossop and K. Ingersent, *Phys. Rev. B* **75**, 104410 (2007).
- [25] I. Paul, C. Pépin, and M. R. Norman, *Phys. Rev. Lett.* **98**, 026402 (2007).
- [26] C. Pépin, *Phys. Rev. Lett.* **98**, 206401 (2007).
- [27] L. Wang, Z. Fu, J. Sun, M. Liu, W. Yi, C. Yi, Y. Luo, Y. Dai, G. Liu, Y. Matsushita, K. Yamaura, L. Lu, J.-G. Cheng, Y.-F. Yang, Y. Shi, and J. L. Luo, *npj Quantum Mater.* **2**, 36 (2017).
- [28] Compared to the previous work in two dimensions [19,20], in Eq. (1) the Ising exchange term has a factor 1/2 difference.
- [29] N. Ishimura and H. Shiba, *Prog. Theor. Phys.* **63**, 743 (1980).
- [30] Q. Si, J.-X. Zhu, and D. R. Grempel, *J. Phys.: Condens. Matter* **17**, R1025 (2005).
- [31] H. Tsujii, E. Tananka, Y. Ode, T. Katoh, T. Mamiya, S. Araki, R. Settai, and Y. Onuki, *Phys. Rev. Lett.* **84**, 5407 (2000).
- [32] A. M. Tselik, *Phys. Rev. Lett.* **72**, 1048 (1994).
- [33] H. Tsunetsugu, Y. Hatsugai, K. Ueda, and M. Sigrist, *Phys. Rev. B* **46**, 3175 (1992).
- [34] C. C. Yu and S. R. White, *Phys. Rev. Lett.* **71**, 3866 (1993).
- [35] N. Shibata, T. Nishino, K. Ueda, and C. Ishii, *Phys. Rev. B* **53**, R8828(R) (1996).
- [36] N. Shibata and K. Ueda, *J. Phys.: Condens. Matter* **11**, R1 (1999).
- [37] S. R. White, *Phys. Rev. Lett.* **69**, 2863 (1992).
- [38] T. D. Kühner and S. R. White, *Phys. Rev. B* **60**, 335 (1999).
- [39] E. Jeckelmann, *Phys. Rev. B* **66**, 045114 (2002).
- [40] J.-X. Zhu, J.-P. Julien, Y. Dubi, and A. V. Balatsky, *Phys. Rev. Lett.* **108**, 186401 (2012).
- [41] J.-X. Zhu, I. Martin, and A. R. Bishop, *Phys. Rev. Lett.* **100**, 236403 (2008).
- [42] T. Senthil, M. Vojta, and S. Sachdev, *Phys. Rev. B* **69**, 035111 (2004).
- [43] E. Novais, E. Miranda, A. H. Castro Neto, and G. G. Cabrera, *Phys. Rev. B* **66**, 174409 (2002).